Ab initio calculations of $BaTiO_3$ and $PbTiO_3$ (001) and (011) surface structures

R. I. Eglitis, and David Vanderbilt
Department of Physics and Astronomy, Rutgers University,
136 Frelinghuysen Road, Piscataway, New Jersey 08854-8019, USA
(Dated: October 3, 2007)

We present and discuss the results of calculations of surface relaxations and rumplings for the (001) and (011) surfaces of $BaTiO_3$ and $PbTiO_3$, using a hybrid B3PW description of exchange and correlation. On the (001) surfaces, we consider both AO (A = Ba or Pb) and TiO_2 terminations. In the former case, the surface AO layer is found to relax inward for both materials, while outward relaxations of all atoms in the second layer are found at both kinds of (001) terminations and for both materials. The surface relaxation energies of BaO and TiO_2 terminations on $BaTiO_3$ (001) are found to be comparable, as are those of PbO and TiO_2 on $PbTiO_3$ (001), although in both cases the relaxation energy is slightly larger for the TiO_2 termination. As for the (011) surfaces, we consider three types of surfaces, terminating on a TiO layer, a Ba or Pb layer, or an O layer. Here, the relaxation energies are much larger for the TiO-terminated than for the Ba or Pb-terminated surfaces. The relaxed surface energy for the O-terminated surface is about the same as the corresponding average of the TiO and Pb-terminated surfaces on $PbTiO_3$, but much less than the average of the TiO and Ba-terminated surfaces on $BaTiO_3$. We predict a considerable increase of the Ti-O chemical bond covalency near the $BaTiO_3$ and $PbTiO_3$ (011) surface as compared to both the bulk and the (001) surface.

PACS numbers: 68.35.bt, 68.35.Md, 68.47.Gh

I. INTRODUCTION

Thin films of ABO_3 perovskite ferroelectrics play an important role in numerous microelectronic, catalytic, and other high-technology applications, and are frequently used as substrates for growth of other materials such as cuprate superconductors.[1,2] Therefore, it is not surprising that a large number of *ab initio* quantum mechanical calculations,[3,4,5,6,7,8,9,10,11,12,13] as well as several classical shell-model (SM) studies,[14,15,16] have dealt with the atomic and electronic structure of the (001) surface of $BaTiO_3$, $PbTiO_3$, and $SrTiO_3$ crystals. In order to study the dependence of the surface relaxation properties on the exchange-correlation functionals and the type of basis (localized vs. plane-wave) used in the calculations, a detailed comparative study of $SrTiO_3$ (001) surfaces based on ten different quantum-mechanical techniques[17,18] was recently performed.

Due to intensive development and progressive miniaturization of electronic devices, the surface structure as well as the electronic properties of the ABO_3 perovskite thin films have been extensively studied experimentally during the last years. The $SrTiO_3$ (001) surface structure has been analyzed by means of low-energy electron diffraction (LEED),[19] reflection high-energy electron diffraction (RHEED),[20] X-ray photoelectron spectroscopy (XPS), ultraviolet electron spectroscopy (UPS), medium-energy ion scattering (MEIS),[21] and surface X-ray diffraction (SXRD).[22] Nevertheless it is important to note that the LEED[19] and RHEED[20] experiments contradict each other in the sign (contraction or expansion) of the interplanar distance between top metal atom and the second crystal layer for the SrO-terminated $SrTiO_3$ (001) surface. The most recent experimental studies on the $SrTiO_3$ surfaces include a combination of XPS, LEED, and time-of-flight scattering and recoil spectrometry (TOF-SARS),[23] as well as metastable impact electron spectroscopy (MIES).[24] In these recent studies, well-resolved 1×1 LEED patterns were obtained for the TiO_2-terminated $SrTiO_3$ (001) surface. Simulations of the TOF-SARS azimuthal scans indicate that the O atoms are situated 0.1 Å above the Ti layer (surface plane) in the case of the TiO_2-terminated $SrTiO_3$ (001) surface.

While the (001) surfaces of $SrTiO_3$, $BaTiO_3$ and $PbTiO_3$ have been extensively studied, much less is known about the (011) surfaces. The scarcity of information about these surfaces is likely due to the polar character of the (011) orientation. (011) terminations of $SrTiO_3$ have frequently been observed, but efforts towards the precise characterization of their atomic-scale structure and corresponding electronic properties has only begun in the last decade, specifically using atomic-force microscopy,[25] scanning tunneling microscopy (STM), Auger spectroscopy, and low-energy electron-diffraction (LEED)[26] methods.

To the best of our knowledge, very few *ab initio* studies of perovskite (011) surfaces exist. The first *ab initio* study of the electronic and atomic structures of several (1×1) terminations of the (011) polar orientation of the $SrTiO_3$ surface was performed by Bottin *et al.*[27] One year later Heifets *et al.*[28] performed very comprehensive *ab initio* Hartree-Fock calculations for four possible terminations (TiO, Sr, and two kinds of O terminations) of the $SrTiO_3$ (011) surface. Recently Heifets *et al.*[29] performed *ab initio* density-functional calculations of the atomic structure and charge redistribution for different terminations of the $BaZrO_3$ (011) surfaces. However, despite the high technological potential of $BaTiO_3$ and $PbTiO_3$, we are unaware of any previous *ab initio* cal-

culations performed for the $BaTiO_3$ and $PbTiO_3$ (011) surfaces. In this study, therefore, we have investigated the (011) as well as the (001) surfaces of $BaTiO_3$ and $PbTiO_3$, with an emphasis on the effect of the surface relaxation and rumpling, surface energies, and the charge redistributions and changes in bond strength that occur at the surface.

II. PRELIMINARIES

A. Computational method

We carry out first-principles calculations in the framework of density-functional theory (DFT) using the CRYSTAL computer code.[30] Unlike the plane-wave codes employed in many previous studies,[31,32] CRYSTAL uses localized Gaussian-type basis sets. In our calculations, we adopted the basis sets developed for $BaTiO_3$ and $PbTiO_3$ in Ref. [33]. Our calculations were performed using the hybrid exchange-correlation B3PW functional involving a mixture of non-local Fock exact exchange, LDA exchange, and Becke's gradient corrected exchange functional,[34] combined with the non-local gradient corrected correlation potential of Perdew and Wang.[35,36,37] We chose the hybrid B3PW functional for our current study because it yields excellent results for the $SrTiO_3$, $BaTiO_3$, and $PbTiO_3$ bulk lattice constant and bulk modulus.[17,33]

The reciprocal-space integration was performed by sampling the Brillouin zone with an 8×8×8 Pack-Monkhorst mesh,[38] which provides a balanced summation in direct and reciprocal spaces. To achieve high accuracy, large enough tolerances of 7, 8, 7, 7, and 14 were chosen for the dimensionless Coulomb overlap, Coulomb penetration, exchange overlap, first exchange pseudo-overlap, and second exchange pseudo-overlap parameters, respectively.[30]

An advantage of the CRYSTAL code is that it treats isolated 2D slabs, without any artificial periodicity in the z direction perpendicular to the surface, as commonly employed in most previous surface band-structure calculations (e.g., Ref. [8]). In the present *ab initio* investigation, we have studied several isolated periodic two-dimensional slabs of cubic $BaTiO_3$ and $PbTiO_3$ crystals containing 7 planes of atoms.

B. Surface geometries

The $BaTiO_3$ and $PbTiO_3$ (001) surfaces were modeled using symmetric (with respect to the mirror plane) slabs consisting of seven alternating TiO_2 and BaO or PbO layers, respectively. One of these slabs was terminated by BaO planes for the $BaTiO_3$ crystal (or PbO planes for $PbTiO_3$) and consisted of a supercell containing 17 atoms. The second slab was terminated by TiO_2 planes for both materials and consisted of a supercell containing 18 atoms. These slabs are non-stoichiometric, with unit cell formulae $Ba_4Ti_3O_{10}$ or $Pb_4Ti_3O_{10}$, and $Ba_3Ti_4O_{11}$ or $Pb_3Ti_4O_{11}$ for $BaTiO_3$ and $PbTiO_3$ perovskites, respectively. These two (BaO or PbO and TiO_2) terminations are the only two possible flat and dense (001) surfaces for the $BaTiO_3$ or $PbTiO_3$ perovskite lattice structure. The sequence of layers at the TiO_2-terminated (001) surface of $BaTiO_3$ is illustrated in Fig. 1.

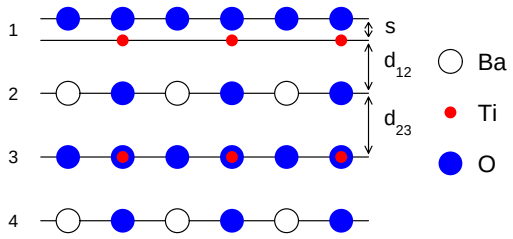

FIG. 1: (Color online.) Side view of a TiO_2-terminated $BaTiO_3$ (001) surface with the definitions of the surface rumpling s and the near-surface interplanar distances d_{12} and d_{23}, respectively.

Unlike the (001) cleavage of $BaTiO_3$ or $PbTiO_3$, which naturally gives rise to non-polar BaO (or PbO) and TiO_2 terminations, a naive cleavage of $BaTiO_3$ or $PbTiO_3$ to create (011) surfaces leads to the formation of polar surfaces. For example, the stacking of the $BaTiO_3$ crystal along the (011) direction consists of alternating planes of O_2 and BaTiO units having nominal charges of $-4e$ and $+4e$ respectively, assuming O^{2-}, Ti^{4+}, and Ba^{2+} constituents. (Henceforth we shall use $BaTiO_3$ for presentation purposes, but everything that is said will apply equally to the $PbTiO_3$ case.) Thus, a simple cleavage leads to O_2-terminated and BaTiO-terminated (011) surfaces that are *polar* and have nominal surface charges of $-2\,e$ and $+2\,e$ per surface cell respectively. These are shown as the top and bottom surfaces in Fig. 2(a) respectively. If uncompensated, the surface charge would lead to an infinite electrostatic cleavage energy. In reality, the polar surfaces would probably become metallic in order to remain neutral, but in view of the large electronic gaps in the perovskites, such metallic surfaces would presumably be unfavorable. Thus, we may expect rather generally that such polar crystal terminations are relatively unstable in this class of materials.[3]

On the other hand, if the cleavage occurs in such a way as to leave a half layer of O_2 units on each surface, we obtain the non-polar surface structure shown in Fig. 2(b). Every other surface O atom has been removed, and the remaining O atoms occupy the same sites as in the bulk structure. We shall refer to this as the "O-terminated" (011) surface, in distinction to the "O_2-terminated" polar surface already discussed in Fig. 2(a). The non-polar nature of the O-terminated surface can be confirmed by noting that the 7-layer 15-atom $Ba_3Ti_3O_9$ slab shown in Fig. 2(b), which has two O-terminated surfaces, is neutral. It is also possible to make non-polar TiO-terminated and Ba-terminated surfaces, as shown in Figs. 2(c) and

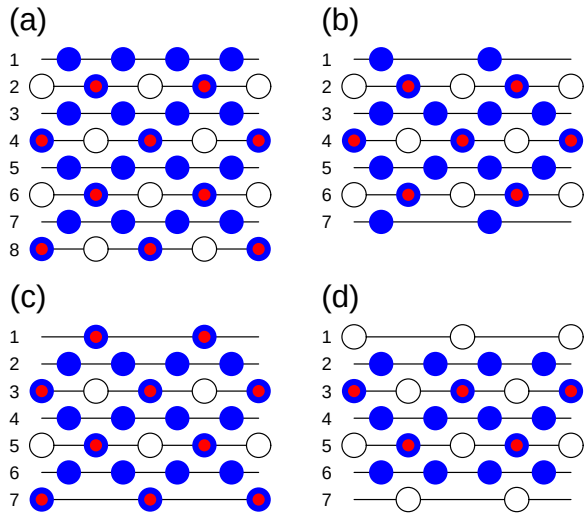

FIG. 2: (Color online.) Side views of slab geometries used to study $BaTiO_3$ (011) surfaces. (a) Stoichiometric 8-layer slab with O_2-terminated and BaTiO-terminated surfaces at top and bottom respectively. (b) 7-layer slab with O-terminated surfaces. (c) 7-layer slab with TiO-terminated surfaces. (d) 7-layer slab with Ba-terminated surfaces.

(d), respectively. This is accomplished by splitting a BaTiO layer during cleavage, instead of splitting an O_2 layer. For the TiO and Ba-terminated surfaces, we use 7-layer slabs having composition $Ba_2Ti_4O_{10}$ (16 atoms) and $Ba_4Ti_2O_8$ (14 atoms) as shown in Fig. 2(c-d), respectively. These are again neutral, showing that the surfaces are non-polar (even though they no longer have precisely the bulk $BaTiO_3$ stoichiometry).

III. RESULTS OF CALCULATIONS

A. $BaTiO_3$ and $PbTiO_3$ (001) surface structure

In the present calculations of the $BaTiO_3$ and $PbTiO_3$ (001) surface atomic structure, we allowed the atoms located in the two outermost surface layers to relax along the z-axis (the forces along the x and y-axes are zero by symmetry). Here we use the term "layer" to refer to a BaO, PbO, or TiO_2 plane, so that there are two layers per stacked unit cell. For example, on the BaO or PbO-terminated surfaces, the top layer is BaO or PbO and the second layer is TiO_2; displacements of the third-layer atoms were found to be negligibly small in our calculations and thus were neglected.

The calculated atomic displacements for the TiO_2 and BaO-terminated (001) surfaces of $BaTiO_3$, and for the TiO_2 and PbO-terminated (001) surfaces of $PbTiO_3$, are presented in Table I. For $BaTiO_3$ (001), comparisons are also provided with the surface atomic displacements obtained by Padilla and Vanderbilt[4] using plane-wave DFT methods in the local-density approximation (LDA), and by Heifets *et al.* using a classical shell-model (SM) approach.[16] Similarly, for $PbTiO_3$ (001), Table I shows comparisons with the plane-wave LDA calculations of Meyer and Vanderbilt.[5] The relaxation of the surface metal atoms in both the $BaTiO_3$ and $PbTiO_3$ surfaces is much larger than that of the oxygen ions, leading to a considerable surface rumpling, which we quantify via a parameter s defined as the relative displacement of the oxygen with respect to the metal atom in a given layer. The surface rumpling and relative displacements of three near-surface planes are presented in Table II. According to our calculations, atoms of the first surface layer relax inwards (i.e., towards the bulk) for BaO and PbO terminations of both materials. Our calculations are in a qualitative agreement with the *ab initio* calculations performed by Padilla and Vanderbilt[4] for $BaTiO_3$, and by Meyer and Vanderbilt[5] for $PbTiO_3$. However, the predictions of the SM calculation disagree with the first-principles calculations; the SM predicts that the first-layer oxygen ions relax outward on the BaO-terminated $BaTiO_3$ (001) surface,[16] rather than inwards. However, the magnitudes of the displacements are relatively small (-0.63% of the lattice constant a_0 in this study and 1.00% of a_0 in the SM calculations)[16] which may be close to the error bar of the classical shell model. Outward relaxations of all atoms in the second layer are found at both (001) terminations of the $BaTiO_3$ and $PbTiO_3$ surfaces. From Table I, we can conclude that the magnitudes of the atomic displacements calculated using different *ab initio* methods and using the classical shell model are in a reasonable agreement.

In order to compare the calculated surface structures further with experimental results, the surface rumpling s and the changes in interlayer distances Δd_{12} and Δd_{23}, as defined in Fig. 1, are presented in Table II. Our calculations of the interlayer distances are based on the positions of relaxed metal ions, which are known to be much stronger electron scatters that the oxygen ions.[19]

For $BaTiO_3$ (001), the rumpling of TiO_2-terminated surface is predicted to exceed that of BaO-terminated surface by a factor of two. This finding is in line with the values of surface rumpling reported by Padilla and Vanderbilt.[4] In contrast, $PbTiO_3$ demonstrates practically the same rumpling for both terminations. From Table II one can see that qualitative agreement between all theoretical methods is obtained. In particular, the relaxed (001) surface structure shows a reduction of interlayer distance Δd_{12} and an expansion of Δd_{23} according to all *ab initio* and shell-model results.

As for experimental confirmation of these results, we are unfortunately unaware of experimental measurements of Δd_{12} and Δd_{23} for the $BaTiO_3$ and $PbTiO_3$ (001) surfaces. Moreover, for the case of the SrO-terminated $SrTiO_3$ (001) surface, existing LEED[19] and RHEED[20] experiments actually contradict each other regarding the sign of Δd_{12}. In view of the absence of clear experimental determinations of these parameters, therefore, the first-principles calculations are a particularly important tool for understanding the surface properties.

TABLE I: Vertical atomic relaxations (in percent of bulk lattice constant) for $BaTiO_3$ and $PbTiO_3$ (001) surfaces. Positive sign corresponds to outward atomic displacement. 'SM' indicates shell-model calculation of Ref. [16]; 'LDA' are previous calculations of Ref. [4] and [5] for $BaTiO_3$ and $PbTiO_3$ respectively.

$BaTiO_3$ (001) surface relaxations						$PbTiO_3$ (001) surface relaxations				
Termination	Layer	Ion	This study	SM	LDA	Termination	Layer	Ion	This study	LDA
BaO	1	Ba	−1.99	−3.72	−2.79	PbO	1	Pb	−3.82	−4.36
		O	−0.63	1.00	−1.40			O	−0.31	−0.46
	2	Ti	1.74	1.25	0.92		2	Ti	3.07	2.39
		O	1.40	0.76	0.48			O	2.30	1.21
	3	Ba		−0.51	0.53		3	Pb		−1.37
		O		0.16	0.26			O		−0.20
TiO_2	1	Ti	−3.08	−2.72	−3.89	TiO_2	1	Ti	−2.81	−3.40
		O	−0.35	−0.94	−1.63			O	0.31	−0.34
	2	Ba	2.51	2.19	1.31		2	Pb	5.32	4.53
		O	0.38	−0.17	−0.62			O	1.28	0.43
	3	Ti		−0.33	−0.75		3	Ti		−0.92
		O		−0.01	−0.35			O		−0.27

B. $BaTiO_3$ and $PbTiO_3$ (011) surface structure

To our knowledge, we have performed the first *ab initio* calculations for $BaTiO_3$ and $PbTiO_3$ (011) surfaces. We have studied the TiO_2-terminated, BaO or PbO-terminated, and O-terminated surfaces illustrated in Fig. 2(c), (d), and (b), respectively. The computed surface atomic relaxations are reported in Table III.

Focusing first on the $BaTiO_3$ surfaces, we find that the Ti ions in the outermost layer of the TiO-terminated surface move inwards (towards the bulk) by $0.0786\,a_0$, whereas the O ions in the outermost layer move outwards by a $0.0261\,a_0$. The Ba atoms in the top layer of the Ba-terminated surface of Fig. 2(d) and the O atoms in the outermost layer of O-terminated surface of Fig. 2(b) move inwards by $0.0867\,a_0$ and $0.0540\,a_0$, respectively. The agreement between our *ab initio* B3PW and the classical SM calculations is satisfactory for all three of these surface terminations. In particular, the directions of the displacements of first and second-layer atoms coincide for all three terminations. This indicates that classical SM calculations with a proper parameterization can serve as a useful initial approximation for modeling the atomic structure in perovskite thin films.

Turning now to our results for the $PbTiO_3$ (011) surfaces, we find that all metal atoms in the outermost layer move inwards irrespective of the termination. Surface oxygen atoms are displaced outwards for the TiO-terminated surface, while oxygen atoms move inwards in the O-terminated surface. The displacement patterns of atoms in the outermost surface layers are similar to those of the $BaTiO_3$ (011) surfaces, as well as classical shell model results for $BaTiO_3$.[16] For example, the atomic displacement magnitudes of Ti and oxygen atoms in the TiO-terminated $PbTiO_3$ (011) surface are $-0.0813\,a_0$ and $0.033\,a_0$ respectively. The Pb atom is displaced inwards by $0.1194\,a_0$ for the Pb-terminated surface, similar to the corresponding $BaTiO_3$ case. Overall, Table III shows similar displacement patterns for the $BaTiO_3$ and $PbTiO_3$ (011) surfaces, as well as qualitatively similar results for both ab initio and classical shell-model descriptions.

TABLE II: Calculated surface rumpling s and interlayer displacements Δd_{ij} (in percent of bulk lattice constant) for near-surface planes on the BaO or PbO and TiO_2-terminated (001) surfaces of $BaTiO_3$ and $PbTiO_3$.

	BaO or PbO term.			TiO_2 termination		
	s	Δd_{12}	Δd_{23}	s	Δd_{12}	Δd_{23}
$BaTiO_3$ (001)						
This study	1.37	−3.74	1.74	2.73	−5.59	2.51
LDA, Ref.4	1.39	−3.71	0.39	2.26	−5.20	2.06
SM, Ref.16	4.72	−4.97	1.76	1.78	−4.91	2.52
$PbTiO_3$ (001)						
This study	3.51	−6.89	3.07	3.12	−8.13	5.32
LDA, Ref.5	3.9	−6.75	3.76	3.06	−7.93	5.45

C. $BaTiO_3$ and $PbTiO_3$ (001) and (011) surface energies

In the present work, we define the unrelaxed surface energy of a given surface termination X to be one half of the energy needed to cleave the crystal rigidly into an unrelaxed surface X and an unrelaxed surface with the complementary termination X'. For $BaTiO_3$, for example, the unrelaxed surface energies of the complementary BaO and TiO_2-terminated (001) surfaces are equal, as are those of the TiO and Ba-terminated (011) surfaces (and similarly for $PbTiO_3$). The relaxed surface energy is defined to be the energy of the unrelaxed surface plus the (negative) surface relaxation energy. These definitions are chosen for consistency with Refs. [17,28]. Unlike the authors of Refs. [27,29], we have made no effort to introduce chemical potentials here, so the results must be used with caution when addressing questions of the

TABLE III: Calculated surface relaxations of $BaTiO_3$ and $PbTiO_3$ (011) surfaces (in percent of the lattice constant) for the three surface terminations. 'SM' indicates comparative results from the shell-model calculation of Ref. [16].

		$BaTiO_3$ (011) surface						$PbTiO_3$ (011) surface	
Layer	Ion	Δz	Δy	Δz (SM)	Δz (SM)	Layer	Ion	Δz	Δy
TiO-terminated						TiO-terminated			
1	Ti	−7.86		−6.93		1	Ti	−8.13	
1	O	2.61		6.45		1	O	3.30	
2	O	−1.02		−1.66		2	O	−0.41	
3	Ba	−0.88		−3.85		3	Pb	−2.54	
3	O			−2.40		3	O	−4.07	
3	Ti			1.59		3	Ti	0.30	
Ba-terminated						Pb-terminated			
1	Ba	−8.67		−13.49		1	Pb	−11.94	
2	O	0.80		2.80		2	O	−0.61	
3	Ti	0.16		−1.20		3	Ti	1.78	
3	O	−0.43		−2.94		3	O	1.67	
3	Ba			2.52		3	Pb	1.52	
O-terminated						O-terminated			
1	O	−5.40	−1.67	−11.16	−6.70	1	O	−7.37	−0.07
2	Ti	−0.15	−6.38	−1.83	−5.33	2	Ti	0.20	−2.54
2	Ba	1.54	−1.27	4.84	−2.21	2	Pb	0.18	−7.50
2	O	1.95	2.97	4.54	5.90	2	O	0.51	2.19
3	O	0.90	4.49	6.52	5.58	3	O	−0.41	3.30

relative stability of surfaces with different stoichiometry.

With these definitions, and using the 7-layer slab geometries specified in Sec. II B, the energy of the unrelaxed $BaTiO_3$ (001) surface is

$$E^{\rm unr}_{\rm surf}(X) = \frac{1}{4}[E^{\rm unr}_{\rm slab}({\rm BaO}) + E^{\rm unr}_{\rm slab}({\rm TiO_2}) - 7E_{\rm bulk}] \quad (1)$$

where X = BaO or TiO_2 specifies the termination, $E^{\rm unr}_{\rm slab}$(BaO) and $E^{\rm unr}_{\rm slab}$(TiO_2) are the unrelaxed BaO and TiO_2-terminated slab energies, $E_{\rm bulk}$ is energy per bulk $BaTiO_3$ unit cell, and the factor of four comes from the fact that four surfaces are created by the two cleavages needed to make the two slabs. The relaxation energy for each termination can be computed from the corresponding slab alone using

$$\Delta E^{\rm rel}_{\rm surf}(X) = \frac{1}{2}[E_{\rm slab}(X) - E^{\rm unr}_{\rm slab}(X)], \quad (2)$$

where $E_{\rm slab}(X)$ is a slab energy after relaxation. The relaxed surface energy is then

$$E_{\rm surf}(X) = E^{\rm unr}_{\rm surf}(X) + \Delta E^{\rm rel}_{\rm surf}(X). \quad (3)$$

Similarly, for the $BaTiO_3$ (011) case, a cleavage on a bulk BaTiO plane gives rise to the complementary TiO and Ba-terminated surfaces shown in Fig. 2(c) and (d) respectively. Thus,

$$E^{\rm unr}_{\rm surf}(X) = \frac{1}{4}[E^{\rm unr}_{\rm slab}({\rm Ba}) + E^{\rm unr}_{\rm slab}({\rm TiO}) - 6E_{\rm bulk}], \quad (4)$$

where the energy is the same for X = TiO or Ba, $E^{\rm unrel}_{\rm slab}$(Ba) and $E^{\rm unrel}_{\rm slab}$(TiO) are energies of the unrelaxed slabs. Relaxation energies can again be computed independently for each slab in a manner similar to Eq. (2). Finally, the (011) surface can also be cleaved to give two identical self-complementary O-terminated surfaces of the kind shown in Fig. 2(b). In this case the 7-layer slab has the stoichiometry of three bulk unit cells, so the relaxed surface energy of the O-terminated (011) surface is

$$E_{\rm surf}(O) = \frac{1}{2}[E_{\rm slab}(O) - 3E_{\rm bulk}], \quad (5)$$

where $E_{\rm slab}(O)$ is the relaxed energy of the slab having two O-terminated surfaces. Everything said here about $BaTiO_3$ surfaces applies in exactly the same way to the corresponding $PbTiO_3$ surfaces.

The calculated surface energies of the relaxed $BaTiO_3$ (001) and (011) surfaces are presented in Table IV. In $BaTiO_3$, the relaxation energies of the TiO_2 and BaO-

TABLE IV: Calculated surface energies for $BaTiO_3$ and $PbTiO_3$ (001) and (011) surfaces (in eV per surface cell). 'SM' indicates comparative results from the shell-model calculation of Ref. [16].

Surface	Termination	$E_{\rm surf}$	$E_{\rm surf}$ (SM)
$BaTiO_3$ (001)	TiO_2	1.07	1.40
	BaO	1.19	1.45
$BaTiO_3$ (011)	TiO	2.04	2.35
	Ba	3.24	4.14
	O	1.72	1.81
$PbTiO_3$ (001)	TiO_2	0.74	
	PbO	0.83	
$PbTiO_3$ (011)	TiO	1.36	
	Pb	2.03	
	O	1.72	

TABLE V: Calculated magnitudes of atomic displacements D (in Å), effective atomic charges Q (in e), and bond populations P between metal-oxygen nearest neighbors (in $10^{-3}e$) for the $BaTiO_3$ and $PbTiO_3$ (001) surfaces.

		$BaTiO_3$ (001) surface				$PbTiO_3$ (001) surface			
Layer	Property	Ion	TiO_2-terminated	Ion	BaO-terminated	Ion	TiO_2-terminated	Ion	PbO-terminated
1	D	Ti	−0.123	Ba	−0.080	Ti	−0.111	Pb	−0.150
	Q		2.307		1.752		2.279		1.276
	P		126		−30		114		54
	D	O	−0.014	O	−0.025	O	0.012	O	−0.012
	Q		−1.280		−1.473		−1.184		−1.128
	P		−38		80		44		106
2	D	Ba	0.101	Ti	0.070	Pb	0.209	Ti	0.121
	Q		1.767		2.379		1.275		2.331
	P		−30		88		8		80
	D	O	0.015	O	0.056	O	0.050	O	0.091
	Q		−1.343		−1.418		−1.167		−1.258
	P		90		−30		80		6
3	Q	Ti	2.365	Ba	1.803	Ti	2.335	Pb	1.358
	P		104		−36		108		24
	Q	O	−1.371	O	−1.417	O	−1.207	O	−1.259
	P		−34		98		18		96
Bulk	Q	Ba	1.797	Ba	1.797	Pb	1.354	Pb	1.354
	P		−34		−34		16		16
	Q	O	−1.388	O	−1.388	O	−1.232	O	−1.232
	P		98		98		98		98
	Q	Ti	2.367	Ti	2.367	Ti	2.341	Ti	2.341

terminated surfaces (−0.23 and −0.11 eV respectively) are comparable, leading to rather similar surface energies. On the (011) surfaces, however, the relaxation energies vary more strongly with termination. For example, we find a relaxation energy of −2.13 eV for the TiO-terminated surface, much larger than −0.93 eV for the Ba-terminated surface. The relaxation energy of −1.15 eV for O-terminated surface gives rise to a relaxed energy of the O-terminated surface (1.72 eV) that is much lower than the average of the TiO and Ba-terminated surfaces (2.64 eV), indicating that it takes much less energy to cleave on an O_2 plane than on a BaTiO plane. The shell-model results of Ref. [16] for the $BaTiO_3$ surfaces are given shown for comparison; the results are qualitatively similar, but there are some significant quantitative differences, especially for the Ba-terminated (011) surface.

The corresponding results are also given for the (001) and (011) surfaces of $PbTiO_3$ in Table IV. The results for the (001) surfaces are similar to those for $BaTiO_3$, although the relaxed surface energies are somewhat lower. For the case of the (011) surfaces, however, we find a different pattern than for $BaTiO_3$. We find a very large relaxation energy of −1.75 eV for the TiO-terminated surface, compared with −1.08 eV for the Pb-terminated surface and −1.12 eV for the O-terminated surface. The average energy of the TiO and Pb-terminated surfaces is now 1.69 eV, to be compared with 1.72 eV for the O-terminated surface, indicating that the cleavage on a PbTiO or an O_2 plane has almost exactly the same energy cost.

D. $BaTiO_3$ and $PbTiO_3$ (001) and (011) surface charge distribution and chemical bonding

To characterize the chemical bonding and covalency effects, we used a standard Mulliken population analysis for the effective static atomic charges Q and other local properties of the electronic structure as described, for example, in Ref. [39,40]. The results are presented in Table V. Our calculated effective charges for bulk $PbTiO_3$ are $+1.354\,e$ for the Pb atom, $+2.341\,e$ for the Ti atom, and $-1.232\,e$ for the O atom. The bond population describing the chemical bonding is +98 me between Ti and O atoms, +16 me between Pb and O atoms, and +2 me between Pb and Ti atoms. Our calculated effective charges for bulk $BaTiO_3$ are $+1.797\,e$ for the Ba atom, $+2.367\,e$ for the Ti atom, and $-1.388\,e$ for the O atom indicate a high degree of $BaTiO_3$ chemical bond covalency. The bond population between Ti and O atoms in $BaTiO_3$ bulk is exactly the same as in $PbTiO_3$, while that between Ba and Ti is slightly negative, suggesting a repulsive interaction between these atoms in the bulk of the $BaTiO_3$ crystal.

For the TiO_2-terminated $BaTiO_3$ and $PbTiO_3$ (001) surfaces, the major effect observed here is a strengthening of the Ti-O chemical bond near the $BaTiO_3$ and $PbTiO_3$ (001) surfaces, which was already pronounced for the both materials in the bulk. Note that the Ti and O effective charges for bulk $BaTiO_3$ and $PbTiO_3$ are much smaller than those expected in an ionic model ($+4\,e$, and $-2\,e$), and that the Ti-O chemical bonds in bulk $BaTiO_3$ and $PbTiO_3$ are fairly heavily populated

TABLE VI: The A-B bond populations P (in $10^{-3}e$) and interatomic distances R (in Å) on (011) surfaces of $BaTiO_3$ and $PbTiO_3$. Symbols I-IV denote the number of each plane enumerated from the surface. The nearest-neighbor Ti-O distance is 2.004 Å and 1.968 Å in bulk $BaTiO_3$ and $PbTiO_3$, respectively.

$BaTiO_3$ (011) surface				$PbTiO_3$ (011) surface			
Atom A	Atom B	P	R	Atom A	Atom B	P	R
TiO-terminated				TiO-terminated			
Ti(I)	O(I)	130	2.047	Ti(I)	O(I)	132	2.019
	O(II)	198	1.784		O(II)	196	1.766
O(II)	Ti(III)	112	2.009	O(II)	Ti(III)	120	1.948
	Ba(III)	−24	2.808		Pb(III)	24	2.826
	O(III)	−26	2.837		O(III)	−20	2.857
Ti(III)	Ba(III)	−2	3.471	Ti(III)	Pb(III)	2	3.410
	O(III)	118	2.004		O(III)	108	1.975
	O(IV)	96	2.004		O(IV)	88	1.976
Ba(III)	O(III)	−32	2.834	Pb(III)	O(III)	20	2.783
	O(IV)	−38	2.816		O(IV)	8	2.734
O(III)	O(IV)	−30	2.834	O(III)	O(IV)	−36	2.706
Ba-terminated				Pb-terminated			
Ba(I)	O(II)	−38	2.664	Pb(I)	O(II)	126	2.589
O(II)	Ba(III)	−36	2.850	O(II)	Pb(III)	24	2.742
	Ti(III)	84	2.022		Ti(III)	74	1.902
	O(III)	−38	2.859		O(III)	−46	2.739
Ba(III)	O(III)	−36	2.834	Pb(III)	O(III)	−10	2.783
	O(IV)	−36	2.834		O(IV)	36	2.813
Ti(III)	O(III)	76	2.004	Ti(III)	O(III)	62	1.968
	Ba(III)	−2	3.471		Pb(III)	0	3.408
	O(IV)	98	2.008		O(IV)	92	2.018
O(III)	O(IV)	−46	2.825	O(III)	O(IV)	−46	2.816
O-terminated				O-terminated			
O(I)	Ba(II)	−26	2.697	O(I)	Pb(II)	50	2.503
	Ti(II)	168	1.722		Ti(II)	128	1.694
	O(II)	−24	2.801		O(II)	−26	2.689
Ba(II)	O(II)	−40	2.664	Pb(II)	O(II)	78	2.574
	Ti(II)	−2	3.306		Ti(II)	4	3.094
Ti(II)	O(II)	82	2.040	Ti(II)	O(II)	92	1.977
	O(III)	112	1.689		O(III)	126	1.831
O(II)	O(III)	−12	2.825	O(II)	O(III)	−24	2.779
Ba(II)	O(III)	−10	2.968	Pb(II)	O(III)	26	2.716
O(III)	O(IV)	−14	2.945	O(III)	O(IV)	−42	2.842
	Ti(IV)	60	2.159		Ti(IV)	60	2.051
	Ba(IV)	−24	2.767		Pb(IV)	−2	2.712

for both materials.

The Ti-O bond population for the TiO_2-terminated $BaTiO_3$ and $PbTiO_3$ (001) surfaces are $+126\,me$ and $+114\,me$ respectively, which is about 20% larger than the relevant value in the bulk. In contrast, the Pb-O bond population of $+54\,me$) is small for the PbO-terminated $PbTiO_3$ (001) surface, and the Ba-O bond population of $-30\,me$ is even negative for the BaO-terminated $BaTiO_3$ (001) surface, indicating a repulsive character. The effect of the difference in the chemical bonding is also well seen from the Pb and Ba effective charges in the first surface layer, which are close to the formal ionic charge of $+2\,e$ only in the case of the $BaTiO_3$ crystal.

The interatomic bond populations for three possible

TABLE VII: Calculated Mulliken atomic charges Q (in e) and changes in atomic charges ΔQ with respect to the bulk charges (in e) on (011) surfaces of $BaTiO_3$ and $PbTiO_3$. for three terminations. The Mulliken charges are $2.341\,e$ for Ti, $-1.232\,e$ for O, and $1.354\,e$ for Pb in bulk $PbTiO_3$, and $2.367\,e$ for Ti, $-1.388\,e$ for O, and $1.797\,e$ for Ba in bulk $BaTiO_3$.

$BaTiO_3$ (011) surface			$PbTiO_3$ (011) surface		
Atom	Q	ΔQ	Atom	Q	ΔQ
TiO-terminated			TiO-terminated		
Ti(I)	2.216	−0.151	Ti(I)	2.212	−0.129
O(I)	−1.316	0.072	O(I)	−1.261	−0.029
O(II)	−1.155	0.233	O(II)	−1.057	0.175
Ba(III)	1.757	−0.04	Pb(III)	1.253	−0.101
Ti(III)	2.353	−0.014	Ti(III)	2.328	−0.013
O(III)	−1.299	0.089	O(III)	−1.18	0.052
O(IV)	−1.402	−0.014	O(IV)	−1.239	−0.007
Ba−terminated			Pb−terminated		
Ba(I)	1.636	−0.161	Pb(I)	1.122	−0.232
O(II)	−1.483	−0.095	O(II)	−1.140	0.092
Ba(III)	1.799	0.002	Pb(III)	1.340	−0.014
Ti(III)	2.368	0.001	Ti(III)	2.343	0.002
O(III)	−1.446	−0.058	O(III)	−1.277	−0.045
O(IV)	−1.392	−0.004	O(IV)	−1.247	−0.015
O−terminated			O−terminated		
O(I)	−1.158	0.23	O(I)	−1.011	0.221
Ba(II)	1.766	−0.031	Pb(II)	1.257	−0.097
Ti(II)	2.213	−0.154	Ti(II)	2.237	−0.104
O(II)	−1.452	−0.064	O(II)	−1.261	−0.029
O(III)	−1.317	0.071	O(III)	−1.215	0.017
Ba(IV)	1.792	−0.005	Pb(IV)	1.355	0.001
Ti(IV)	2.317	−0.05	Ti(IV)	2.317	−0.024
O(IV)	−1.407	−0.019	O(IV)	−1.233	−0.001

$BaTiO_3$ and $PbTiO_3$ (011) surface terminations are given in Table VI. The major effect observed here is a strong increase of the Ti-O chemical bonding near the $BaTiO_3$ and $PbTiO_3$ (011) surface as compared to already large bonding near the (001) surface ($+126\,me$ and $+114\,me$, respectively) and in the bulk ($+98\,me$). For the O-terminated (011) surface the O(I)–Ti(II) bond population is as large as $+168\,me$ for $BaTiO_3$ and $+128\,me$ for $PbTiO_3$, i.e., considerably larger than in the bulk and on the (001) surface.

Our calculations demonstrate that for the TiO-terminated $BaTiO_3$ and $PbTiO_3$ (011) surfaces, the Ti-O bond populations are larger in the direction perpendicular to the surface ($+198\,me$ for $BaTiO_3$ and $+196\,me$ for $PbTiO_3$) than in plane ($+130\,me$ for $BaTiO_3$ and $+132\,me$ for $PbTiO_3$). The Ti-O bond populations for the TiO-terminated $PbTiO_3$ (011) surface in the direction perpendicular to the surface is twice as large as the Ti-O bond population in $PbTiO_3$ bulk.

In Table VII we present the calculated Mulliken effective charges Q, and their changes ΔQ with respect to the bulk values, near the surface. We analyzed the charge redistribution between different layers in slabs with all three $BaTiO_3$ and $PbTiO_3$ (011) surface terminations. The charge of the surface Ti atoms in the TiO-terminated

$BaTiO_3$ and $PbTiO_3$ (001) surface is reduced by $0.151\,e$ and $0.129\,e$, respectively. Metal atoms in the third layer lose much less charge. Except in the central layer (and, in the case of $PbTiO_3$, in the subsurface layer), the O ions also reduce their charges, becoming less negative. The largest charge change is observed for $BaTiO_3$ and $PbTiO_3$ subsurface O atoms ($+0.233\,e$ and $+0.175\,e$, respectively). This gives a large positive change of $+0.466\,e$ and $+0.350\,e$ in the charge for each $BaTiO_3$ and $PbTiO_3$ subsurface layer.

On the Ba-terminated and Pb-terminated $BaTiO_3$ and $PbTiO_3$ (011) surface, negative changes in the charge are observed for all atoms except for Ba and Ti in the $BaTiO_3$ third layer, Ti atom in the $PbTiO_3$ third layer, and subsurface oxygen atom in $PbTiO_3$. The largest charge changes are at the surface Ba and Pb ions. It is interesting to notice that, due to the tiny difference in the chemical bonding between $BaTiO_3$ and $PbTiO_3$ perovskites, the charge change for the $BaTiO_3$ subsurface O ion ($-0.095\ e$) and $PbTiO_3$ subsurface O ion ($+0.092\,e$) have practically the same magnitude, but opposite signs.

For the O-terminated $BaTiO_3$ and $PbTiO_3$ (011) surfaces, the largest calculated changes in the charge are observed for the $BaTiO_3$ and $PbTiO_3$ surface O atom ($+0.230\,e$ and $+0.221\,e$, respectively). The change of the total charge in the second layer is negative and almost equal for both materials. For the $BaTiO_3$ crystal, this reduction by $0.249\,e$ comes mostly from Ti atom ($-0.154\,e$). In the $PbTiO_3$ crystal, the reduction by $0.230\,e$ appears mostly due to a decrease of the Ti atom charge by $0.104\,e$, as well as a reduction of the Pb atom charge by $0.097\,e$.

IV. CONCLUSIONS

In summary, motivated by the scarcity of experimental investigations of the $BaTiO_3$ and $PbTiO_3$ surfaces and the contradictory experimental results obtained for the related $SrTiO_3$ surface,[19,20] we have carried out predictive electronic structure calculation to investigate the surface atomic and electronic structure of the $BaTiO_3$ and $PbTiO_3$ (001) and (011) surfaces. Using a hybrid B3PW approach, we have calculated the surface relaxation of the two possible terminations (TiO_2 and BaO or PbO) of the $BaTiO_3$ and $PbTiO_3$ (001) surfaces, and three possible terminations (TiO, Ba or Pb, and O) of the $BaTiO_3$ and $PbTiO_3$ (011) surfaces. The data obtained for the surface structures are in a good agreement with previous LDA calculations of Padilla and Vanderbilt,[4] the LDA plane-wave calculations of Meyer *et al.*,[5] and in fair agreement with the shell-model calculations of Heifets *et al.*[16]

According to our calculations, atoms of the first surface layer relax inwards for BaO and PbO terminated (001) surfaces of both materials. Outward relaxations of all atoms in the second layer are found at both terminations of $BaTiO_3$ and $PbTiO_3$ (001) surfaces. In $BaTiO_3$, the rumpling of the TiO_2-terminated (001) surface is predicted to exceed that of the BaO-terminated (001) surface by a factor of two. In contrast, $PbTiO_3$ exhibits practically the same rumplings for both (TiO_2 and PbO) terminations. Our calculated surface energies show that the TiO_2-terminated (001) surface is slightly more stable for both materials than the BaO or PbO-terminated (001) surface. The O-terminated $BaTiO_3$ and TiO-terminated $PbTiO_3$ (011) surfaces have surface energies close to that of the (001) surface. Our calculations suggest that the most unfavorable (011) surfaces are the Ba or Pb-terminated ones for both the $BaTiO_3$ and $PbTiO_3$ cases. We found that relaxation of the $BaTiO_3$ and $PbTiO_3$ surfaces for is considerably stronger for all three (011) terminations than for the (001) surfaces. The atomic displacements in the third plane from the surface for the three terminations of $BaTiO_3$ and $PbTiO_3$ (011) surfaces are still large. Finally, our *ab initio* calculations indicate a considerable increase of Ti-O bond covalency near the $BaTiO_3$ and $PbTiO_3$ (011) surface relative to $BaTiO_3$ and $PbTiO_3$ bulk, much larger than for the (001) surface.

V. ACKNOWLEDGMENTS

The present work was supported by Deutsche Forschungsgemeinschaft (DFG) and by ONR Grant N00014-05-1-0054.

[1] J. F. Scott, *Ferroelectric Memories* (Springer, Berlin, 2000).
[2] M. E. Lines, and A. M. Glass, *Principles and Applications of Ferroelectrics and Related Materials* (Clarendon, Oxford, 1977).
[3] C. Noguera, *Physics and Chemistry at Oxide Surfaces* (Cambridge Univ. Press, N. Y., 1996).
[4] J. Padilla, and D. Vanderbilt, Phys. Rev. B **56**, 1625 (1997).
[5] B. Meyer, J. Padilla, and D. Vanderbilt, Faraday Discussions **114**, 395 (1999).
[6] F. Cora, and C. R. A. Catlow, Faraday Discussions **114**, 421 (1999).
[7] L. Fu, E. Yashenko, L. Resca, and R. Resta, Phys. Rev. B **60**, 2697 (1999).
[8] C. Cheng, K. Kunc, and M. H. Lee, Phys. Rev. B **62**, 10409 (2000).
[9] B. Meyer, and D. Vanderbilt, Phys. Rev. B **63**, 205426 (2001).
[10] C. Bungaro, and K. M. Rabe, Phys. Rev. B **71**, 035420 (2005).
[11] M. Krcmar, and C. L. Fu, Phys. Rev. B **68**, 115404 (2003).
[12] Y. Umeno, T. Shimada, T. Kitamura, C. Elsasser, Phys. Rev. B **74**, 174111 (2006).

[13] B. K. Lai, I. Ponamareva, I. A. Kornev, L. Bellaiche, G. J. Salamo, Phys. Rev. B **75**, 085412 (2007).
[14] E. Heifets, S. Dorfman, D. Fuks, E. Kotomin, and A. Gordon, J. Phys.: Cond. Matter **10**, L347 (1998).
[15] S. Tinte, and M. G. Stachiotti, AIP Conf. Proc. **535**, 273 (2000).
[16] E. Heifets, E. Kotomin, and J. Maier, Surf, Sci. **462**, 19 (2000).
[17] E. Heifets, R. I. Eglitis, E. A. Kotomin, J. Maier, and G. Borstel, Phys. Rev. B **64**, 235417 (2001).
[18] E. Heifets, R. I. Eglitis, E. A. Kotomin, J. Maier, and G. Borstel, Surf. Sci. **513**, 211 (2002).
[19] N. Bickel, G. Schmidt, K. Heinz, K. Muller, Phys. Rev. Lett **62**, 2009 (1989).
[20] T. Hikita, T. Hanada, M. Kudo, M. Kawai, Surf. Sci. **287-288**, 377 (1993).
[21] A. Ikeda, T. Nishimura, T. Morishita, Y. Kido, Surf. Sci. **433-435**, 520 (1999).
[22] G. Charlton, S. Brennan, C. A. Muryn, R. McGrath, D. Norman, T. S. Turner, G. Thorthon, Surf. Sci. **457**, L376 (2000).
[23] P. A. W. van der Heide, Q. D. Jiang, Y. S. Kim, J. W. Rabalais, Surf. Sci. **473**, 59 (2001).
[24] W. Maus-Friedrichs, M. Frerichs, A. Gunhold, S. Krischok, V. Kempter, G. Bihlmayer, Surf. Sci. **515**, 499 (2002).
[25] K. Szot, and W. Speier, Phys. Rev. B **60**, 5909 (1999).
[26] J. Brunen, and J. Zegenhagen, Surf. Sci. **389**, 349 (1997).
[27] F. Bottin, F. Finocchi, and C. Noguera, Phys. Rev. B **68**, 035418 (2003).
[28] E. Heifets, W. A. Goddard III, E. A. Kotomin, R. I. Eglitis, and G. Borstel, Phys. Rev. B **69**, 035408 (2004).
[29] E. Heifets, J. Ho, and B. Merinov, Phys. Rev. B **75**, 155431 (2007).
[30] V. R. Saunders, R. Dovesi, C. Roetti, M. Causa, N. M. Harrison, R. Orlando, C. M. Zicovich-Wilson, *CRYSTAL2003 Users Manual* (University of Torino, Torino, 2003).
[31] R. E. Cohen, J. Phys. Chem. Solids **57**, 1393 (1996).
[32] R. E. Cohen, Ferroelectrics **194**, 323 (1997).
[33] S. Piskunov, E. Heifets, R. I. Eglitis, and G. Borstel, Comput. Mat. Sci. **29**, 165 (2004).
[34] A. D. Becke, J. Chem. Phys. **98**, 5648 (1993).
[35] J. P. Perdew, and Y. Wang, Phys. Rev. B **33**, 8800 (1986).
[36] J. P. Perdew, and Y. Wand, Phys. Rev. B **40**, 3399 (1989)
[37] J. P. Perdew, and Y. Wang, Phys. Rev. B **45**, 13244 (1992).
[38] H. J. Monkhorst, and J. D. Pack, Phys. Rev. B **13**, 5188 (1976).
[39] C. R. A. Catlow, and A. M. Stoneham, J. Phys. C: Solid State Phys. **16**, 4321 (1983).
[40] R. C. Bochiccio, and H. F. Reale, J. Phys. B: At. Mol. Opt. Phys. **26**, 4871 (1993).